# Electromagnetic chirality-induced negative refraction with the same amplitude and anti-phase of the two chirality coefficients*

Zhao Shun-Cai(赵顺才)[a)b)c)], Liu Zheng-Dong(刘正东)[a)b)c)†], Zheng Jun(郑 军)[a)b)c)], and Li Gen(黎 根)[a)b)c)]

[a)] *School of Materials Science and Engineering, Nanchang University, Nanchang* 330031, *China*

[b)] *Engineering Research Centre for Nanotechnology, Nanchang University, Nanchang* 330047, *China*

[c)] *Institute of Modern Physics, Nanchang University, Nanchang* 330031, *China*

(Received 24 May 2010; revised manuscript received 28 January 2011)

This paper suggests a scheme of electromagnetic chirality-induced negative refraction utilizing magneto–electric cross coupling in a four-level atomic system. The negative refraction can be achieved with the two chirality coefficients having the same amplitude but the opposite phase, without requiring the simultaneous presence of an electric-dipole and a magnetic-dipole transition near the same transition frequency.

**Keywords:** electromagnetic chirality, negative refraction, same amplitude and anti-phase, chirality coefficients

**PACS:** 78.20.Ci, 42.65.An, 42.50.–p, 81.05.Zx **DOI:** 10.1088/1674-1056/20/6/067802

## 1. Introduction

Negative refraction of light, first predicted to occur in materials with simultaneous negative permittivity and permeability in 1968,[1] has attracted considerable attention during the last decade.[2−7] Materials with a negative refractive index potentially have many surprising and even counterintuitive electromagnetic and optical effects, such as the reversals of both Doppler shift and Cerenkov radiation,[4] amplification of evanescent waves,[8] subwavelength focusing,[8−10] and so on.[11,12] Until now, there have been several approaches to the realization of negative refractive index materials, including artificial composite metamaterials,[13,14] photonic crystal structures,[15] transmission line simulation[16 and chiral media,[17,18] as well as photonic resonant materials (coherent atomic vapour).[19−21] Early proposals for negative refraction required media with both negative permittivity and permeability ($\varepsilon, \mu < 0$) in the frequency range of interest.[1,4] However, the typical transition of magnetic dipole moments are smaller than the transition of electric dipole moments by a factor of the order of the fine structure constant ($\alpha \approx 1/137$). So, it is difficult to obtain negative permeability due to the smaller typical transition of magnetic-dipole moments. Thus, it is difficult to achieve negative refraction in the optical region of the spectrum because of the weakness of the magnetic response. Recently, to alleviate this problem, a chiral route to negative refraction was suggested[17,22−24] without simultaneously negative electric permittivity and magnetic permeability. The key idea is to use a magnetoelectric cross coupling where the medium's electric polarization is coupled to the magnetic field of the wave and the medium's magnetization is coupled to the electric field. Under such conditions, a negative index of refraction can be achieved without the requirement for negative permeability. The medium in which the electric polarization $\boldsymbol{P}$ is coupled to the magnetic field $\boldsymbol{H}$ of an electromagnetic wave and the magnetization $\boldsymbol{M}$ is coupled to the electric field $\boldsymbol{E}$:

$$\boldsymbol{P} = \varepsilon_0 \chi_{\mathrm{e}} \boldsymbol{E} + \frac{\xi_{\mathrm{EH}}}{c} \boldsymbol{H}, \quad \boldsymbol{M} = \frac{\xi_{\mathrm{HE}}}{c\mu_0} \boldsymbol{E} + \chi_{\mathrm{m}} \boldsymbol{H}. \quad (1)$$

Here $\chi_{\mathrm{e}}$ and $\chi_{\mathrm{m}}$, and $\xi_{\mathrm{EH}}$ and $\xi_{\mathrm{HE}}$ are the electric and magnetic susceptibilities, and the complex chirality coefficients, respectively. They lead to additional contributions to the refractive index for one circular polarization[17,23,24]

$$n = \sqrt{\varepsilon\mu - \frac{(\xi_{\mathrm{EH}} + \xi_{\mathrm{HE}})^2}{4}} + \frac{\mathrm{i}}{2}(\xi_{\mathrm{EH}} - \xi_{\mathrm{HE}}). \quad (2)$$

*Project supported by the National Natural Science Foundation of China (Grant Nos. 60768001 and 10464002).

†Corresponding author. E-mail: zscnum1@126.com; lzdgroup@ncu.edu.cn

© 2011 Chinese Physical Society and IOP Publishing Ltd

One typically chooses the phase such that the chirality coefficients are imaginary, if $\xi_{\rm EH} = -\xi_{\rm HE} = {\rm i}\xi$, and equation (2) reads $n = \sqrt{\epsilon\mu} - \xi$. When $\sqrt{\varepsilon\mu}$ is less than $\xi$ ($\xi > 0$), the negative refraction is obtained without requiring both $\varepsilon < 0$ and $\mu < 0$. In this paper, we propose an alternative scheme to realize negative refraction. We demonstrate that electromagnetic chirality-induced negative refraction can be realized when the two chirality coefficients have the same amplitude but the opposite phase, which requires that the chirality coefficients are not only imaginary. All of these current suggestions for negative refraction in left-handedness[25,26] require a strong magnetic dipole transition and a strong electric-dipole transition near the same transition frequency. This requirement puts a stringent constraint on the energy level structure of systems where negative refraction can be achieved. In this article, the electric-dipole and magnetic-dipole transition will occur at different transition frequencies.

The paper is organized as follows. Section 2 establishes the model, and presents expressions for the chirality coefficients and refractive index. Section 3 is devoted to presenting the numerical results and to discussing numerical results. Finally, Section 4 summarizes the conclusions.

## 2. Theoretical model and chirality coefficients

We proceed with a detailed description of electromagnetically induced chiral negative refraction. The four-level configuration of atoms for consideration is shown in Fig. 1. The parity properties of the atomic states are as follows: levels $|1\rangle$, $|2\rangle$ and $|3\rangle$ have the same parity, which is opposite to the parity of level $|4\rangle$. Since the two lower levels $|1\rangle$ and $|2\rangle$ have the same parity, the coherent coupling $\Omega_{\rm pm}$ cannot be electric-dipole, but instead can be achieved through the magnetic-field, and so $\langle 2|\hat{\boldsymbol{\mu}}|1\rangle \neq 0$ where $\hat{\boldsymbol{\mu}}$ is the magnetic-dipole operator. The two upper levels, $|3\rangle$ and $|4\rangle$, have the opposite parity, the coherent coupling $\Omega_{\rm pe}$ should be electric-dipole with $\langle 4|\hat{\boldsymbol{d}}|3\rangle \neq 0$, where $\hat{\boldsymbol{d}}$ is the electric dipole operator. As shown in Fig. 1, three electromagnetic fields are introduced to couple the four states. The electric ($\boldsymbol{E}$) and magnetic ($\boldsymbol{B}$) components of the probe light (corresponding Rabi frequency $\Omega_{\rm pe} = \boldsymbol{E}_{\rm P} \cdot \boldsymbol{d}_{34}/\hbar$, $\Omega_{\rm pm} = \boldsymbol{B}_{\rm P} \cdot \boldsymbol{\mu}_{12}/\hbar$) interact with the transitions $|3\rangle$ and $|4\rangle$ as well as $|2\rangle$ and $|1\rangle$, respectively. Hence, the electric and magnetic components of the probe field with the same frequency $\omega_{\rm p}$ drive the two transitions $|3\rangle$–$|4\rangle$ and $|2\rangle$–$|1\rangle$, simultaneously. The control field with Rabi frequency denoted by $\Omega_{\rm c}$ pumps atoms in level $|1\rangle$ into upper level $|3\rangle$. According to parity selection rules, the transition $|1\rangle$–$|3\rangle$ is assumed to be a two-photon process, as stated in Ref. [19]. The strong signal field couples levels $|2\rangle$ and $|4\rangle$ with Rabi frequency $\Omega_{\rm s}$. In the rotating-wave and dipole approximations, the Hamiltonian of the system can be written as

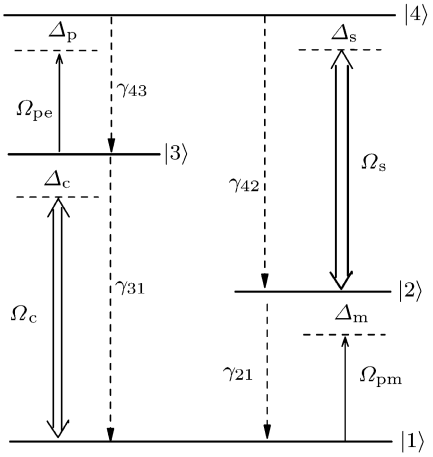



**Fig. 1.** Schematic diagram of a four-level atomic system interacting with the control field having Rabi frequency $\Omega_{\rm c}$, the signal field having Rabi frequency $\Omega_{\rm s}$ and the probe field whose electric and magnetic components are coupled to the level pairs $|4\rangle$–$|3\rangle$ and $|2\rangle$–$|1\rangle$, respectively.

$$\begin{aligned} H = & \sum_{i=1}^{4} \hbar\omega_i |i\rangle\langle i| - \hbar(\Omega_{\rm pm}\, {\rm e}^{-{\rm i}(\omega_{\rm p}t+\theta_{\rm pm})}|2\rangle\langle 1| \\ & + \Omega_{\rm c}\, {\rm e}^{-{\rm i}(2\omega_{\rm c}t+\theta_{\rm c})}|3\rangle\langle 1| + \Omega_{\rm pe}\, {\rm e}^{-{\rm i}(\omega_{\rm p}t+\theta_{\rm pe})}|4\rangle\langle 3| \\ & + \Omega_{\rm s}\, {\rm e}^{-{\rm i}(\omega_{\rm s}t+\theta_{\rm s})}|4\rangle\langle 2| + {\rm c.c.}), \end{aligned} \tag{3}$$

where $\omega_i$ ($i$ = c, s) are the frequencies of the control and signal fields, respectively. $\theta_i$ ($i = {\rm pe}, {\rm pm}, {\rm c}, {\rm s}$) represents phases of the electric and magnetic components of the probe field, control and the signal fields, respectively. When the probe field is weak, i.e. $\Omega_{\rm pe}$, $\Omega_{\rm pm} \ll \Omega_{\rm c} < \Omega_{\rm s}$, we find the first-order perturbation solution of the Liouville equation in the steady state

$$\begin{aligned} \rho_{43} &= \alpha_{\rm EE}\boldsymbol{E} + \alpha_{\rm EH}\boldsymbol{B}, \\ \rho_{21} &= \alpha_{\rm HE}\boldsymbol{E} + \alpha_{\rm HH}\boldsymbol{B}, \end{aligned} \tag{4}$$

where the coefficients $\alpha_{\rm EE}$, $\alpha_{\rm EH}$, $\alpha_{\rm HH}$ and $\alpha_{\rm HE}$ are given by

$$\alpha_{\rm EE} = \frac{A_0\Omega_{\rm c}^2 d_{34}(A_{11}A_{12} + A_{13})}{D_0D_1 + D_2\Omega_{\rm s}^2 + \Omega_{\rm s}^4}, \tag{5}$$

$$\alpha_{\rm EH} = \frac{{\rm e}^{{\rm i}\theta}A_0\mu_{12}\Omega_{\rm c}\Omega_{\rm s}[A_{21}-(\Gamma_2+{\rm i}\Delta_{\rm c})(A_{22}-A_{23}\Omega_{\rm c}^2-\gamma_{31}\Omega_{\rm s}^2)]}{D_0D_1+D_2\Omega_{\rm s}^2+\Omega_{\rm s}^4}, \tag{6}$$

$$\alpha_{\rm HE} = \frac{{\rm e}^{{\rm i}\theta}A_0d_{34}\Omega_{\rm c}\Omega_{\rm s}\{A_{41}(\Gamma_2+{\rm i}\Delta_{\rm c})\Omega_{\rm c}^2+({\rm i}\Delta_{\rm c}-\Gamma_2)[\gamma_{31}\Omega_{\rm s}^2-A_{42}\Omega_{\rm c}^2+({\rm i}\Gamma_6+\Delta_{\rm c}-\Delta_{\rm p})A_{43}]}{D_0D_1+D_2\Omega_{\rm s}^2+\Omega_{\rm s}^4}, \tag{7}$$

$$\begin{aligned}\alpha_{\rm HH} = {} & \frac{A_0\mu_{12}A_{31}({\rm i}\Delta_{\rm c}-\Gamma_2)\{A_{33}[(\Gamma_5+{\rm i}\Delta_{\rm p})A_{32}+\Omega_{\rm c}^2]+A_{32}\Omega_{\rm s}^2\}}{D_0D_1+D_2\Omega_{\rm s}^2+\Omega_{\rm s}^4} \\ & - \frac{A_0\mu_{12}\Omega_{\rm c}^2(\Gamma_2+{\rm i}\Delta_{\rm c})\{(\gamma_{31}-A_{33})[(\Gamma_5+{\rm i}\Delta_{\rm p})A_{32}+\Omega_{\rm c}^2]-(A_{32}+\gamma_{31})\Omega_{\rm s}^2\}}{D_0D_1+D_2\Omega_{\rm s}^2+\Omega_{\rm s}^4},\end{aligned} \tag{8}$$

and

$$\begin{aligned}
A_0 &= \frac{\rm i}{\hbar(\Gamma_2^2\gamma_{31}+\gamma_{31}\Delta_{\rm c}^2+4\Gamma_2\Omega_{\rm c}^2)},\\
A_{11} &= \gamma_{31}(\Gamma_2-{\rm i}\Delta_{\rm c})+2\Gamma_1[\Gamma_3+{\rm i}(\Delta_{\rm c}+\Delta_{\rm p})],\\
A_{12} &= (\Gamma_1+{\rm i}\Delta_{\rm m})[\Gamma_6-{\rm i}(\Delta_{\rm c}-\Delta_{\rm p})]+\Omega_{\rm c}^2,\\
A_{13} &= \Omega_{\rm s}^2[{\rm i}\gamma_{31}\Delta_{\rm c}-\Gamma_2(\gamma_{31}-2\Gamma_6+2{\rm i}\Delta_{\rm c}-2{\rm i}\Delta_{\rm p})],\\
A_{21} &= (\Gamma_2-{\rm i}\Delta_{\rm c})(\Gamma_3+\Gamma_6+2{\rm i}\Delta_{\rm p})\\
&\quad\times(\Gamma_2\gamma_{31}+{\rm i}\gamma_{31}\Delta_{\rm c}+\Omega_{\rm c}^2),\\
A_{23} &= \Gamma_3-\gamma_{31}+\Gamma_6+2{\rm i}\Delta_{\rm p},\\
A_{22} &= \gamma_{31}(\Gamma_1+{\rm i}\Delta_{\rm m})[-\Gamma_3-{\rm i}(\Delta_{\rm c}+\Delta_{\rm p})],\\
A_{31} &= -\Gamma_2\gamma_{31}-{\rm i}\gamma_{31}\Delta_{\rm c}-\Omega_{\rm c}^2,\\
A_{32} &= \Gamma_3+{\rm i}(\Delta_{\rm c}+\Delta_{\rm p}),\\
A_{33} &= \Gamma_6+{\rm i}(\Delta_{\rm p}-\Delta_{\rm c}),\\
A_{41} &= \Gamma_3+\Gamma_6+2{\rm i}\Delta_{\rm p},\\
A_{42} &= \Gamma_3+\gamma_{31}+{\rm i}(\Delta_{\rm c}+\Delta_{\rm p}),\\
A_{43} &= \gamma_{31}(\Delta_{\rm p}-{\rm i}\Gamma_5)+{\rm i}\Omega_{\rm c}^2,\\
D_0 &= (\Gamma_1+{\rm i}\Delta_{\rm m})[\Gamma_6-{\rm i}(\Delta_{\rm c}-\Delta_{\rm p})]+\Omega_{\rm c}^2,\\
D_1 &= (\Gamma_5+{\rm i}\Delta_{\rm p})[\Gamma_3+{\rm i}(\Delta_{\rm c}+\Delta_{\rm p})]+\Omega_{\rm c}^2,\\
D_2 &= ({\rm i}\Gamma_6+\Delta_{\rm c}-\Delta_{\rm p})(\Delta_{\rm p}-{\rm i}\Gamma_5)\\
&\quad+(\Gamma_1+{\rm i}\Delta_{\rm m})[\Gamma_3+{\rm i}(\Delta_{\rm c}+\Delta_{\rm p})]-2\Omega_{\rm c}^2,
\end{aligned}$$

with the coherence damping coefficient given by

$$\begin{aligned}
\Gamma_1 &= \frac{1}{2}(\gamma_1+\gamma_{21})+\gamma_{\rm c},\\
\Gamma_2 &= \frac{1}{2}(\gamma_1+\gamma_{31})+\gamma_{\rm c},\\
\Gamma_3 &= \frac{1}{2}(\gamma_1+\gamma_{42}+\gamma_{43})+\gamma_{\rm c},\\
\Gamma_4 &= \frac{1}{2}(\gamma_{21}+\gamma_{42}+\gamma_{43})+\gamma_{\rm c},\\
\Gamma_5 &= \frac{1}{2}(\gamma_{31}+\gamma_{42}+\gamma_{43})+\gamma_{\rm c},\\
\Gamma_6 &= \frac{1}{2}(\gamma_{31}+\gamma_{21}),
\end{aligned}$$

in which $\gamma_{\rm c}$ denotes the collisional dephasing rate and $\gamma_1 = 0$. The detunings of the applied fields are respectively defined by $\Delta_{\rm p} = \omega_{\rm p}-(\omega_4-\omega_3)$, $\Delta_{\rm c} = 2\omega_{\rm c}-(\omega_3-\omega_1)$, $\Delta_{\rm s} = \omega_{\rm s}-(\omega_4-\omega_2)$, $\Delta_{\rm m} = \omega_{\rm p}-(\omega_2-\omega_1)$ and here we depict the electric-dipole and magnetic-dipole transitions to be different by seting $\Delta_{\rm m} \neq \Delta_{\rm p}$ (i.e., two transition frequencies are not near the same frequency in this atomic system).[20] The relative phase of the signal, control and probe electric fields and probe magnetic field is $\theta = \theta_{\rm pe}+\theta_{\rm c}-\theta_{\rm pm}-\theta_{\rm s}$. It is well known that the phases of the electric and magnetic components of an electromagnetic field are identical in a nonconductor.[27] Hence, in our scheme, $\theta_{\rm pe} = \theta_{\rm pm}$ and the relative phase becomes the phase difference of the control and pump fields, i.e., $\theta = \theta_{\rm c}-\theta_{\rm s}$.

The ensemble electric polarization and magnetization of the atomic medium to the probe field are given by $\boldsymbol{P} = N\boldsymbol{d}_{12}\rho_{21}$ and $\boldsymbol{M} = N\boldsymbol{\mu}_{34}\rho_{43}$, respectively, where $N$ is the density of atoms. Then the coherent cross-coupling between electric and magnetic dipole transitions driven by the electric and magnetic components of the probe field may lead to chirality.[17,23,24] Substituting Eq. (4) into the formula for the ensemble electric polarization and magnetization, we have the relations

$$\boldsymbol{P} = a_1\boldsymbol{E}+a_2\boldsymbol{B}, \quad \boldsymbol{M} = a_3\boldsymbol{E}+a_4\boldsymbol{B}, \tag{9}$$

where

$$\begin{aligned}
a_1 &= Nd_{12}\alpha_{\rm HE}, \quad a_2 = Nd_{12}\alpha_{\rm HH},\\
a_3 &= N\mu_{34}\alpha_{\rm EE}, \quad a_4 = N\mu_{34}\alpha_{\rm EH}.
\end{aligned}$$

Considering both electric and magnetic local field effects,[27,28] we find that $\boldsymbol{E}$ and $\boldsymbol{B}$ in Eq. (9) must be replaced by the local fields

$$\boldsymbol{E}_L = \boldsymbol{E}+\frac{\boldsymbol{P}}{3\varepsilon_0}, \quad \boldsymbol{B}_L = \mu_0\left(\boldsymbol{H}+\frac{\boldsymbol{M}}{3}\right).$$

As a result, we obtain

$$\boldsymbol{P} = \frac{3\varepsilon_0(\mu_0a_2a_1-\mu_0a_3a_2-3a_1)}{\mu_0a_3\alpha_{EB}+3a_1-\mu_0a_4a_1-9\varepsilon_0+3\mu_0\varepsilon_0a_4}\boldsymbol{E}+\frac{-9\mu_0\varepsilon_0a_2}{\mu_0a_3a_2+3a_1-\mu_0a_4a_1-9\varepsilon_0+3\mu_0\varepsilon_0a_4}\boldsymbol{H}, \tag{10}$$

$$\boldsymbol{M} = \frac{9\varepsilon_0 a_3}{\mu_0 a_4 a_1 + 9\varepsilon_0 - \mu_0 a_3 a_2 - 3a_1 - 3\varepsilon_0\mu_0 a_4}\boldsymbol{E} + \frac{3(\mu_0 a_3 a_2 - \mu_0 a_4 a_1 + 3\varepsilon_0\mu_0 a_4)}{\mu_0 a_4 a_1 + 9\varepsilon_0 - \mu_0 a_3 a_2 - 3a_1 - 3\varepsilon_0\mu_0 a_4}\boldsymbol{H}. \quad (11)$$

Comparing Eqs. (10) and (11) with Eq. (1), we obtain the electric permittivity, the magnetic permeability and the complex chirality coefficients as follows:

$$\varepsilon = 1 + \chi_{\rm e} = \frac{6a_1 + 9\varepsilon_0 + \mu_0[2a_3 a_2 - a_4(2a_1 + 3\varepsilon_0)]}{-3a_1 + \mu_0[-a_3 a_2 + a_4(a_1 - 3\varepsilon_0)] + 9\varepsilon_0}, \quad (12)$$

$$\mu = 1 + \chi_{\rm m} = \frac{-3\alpha_1 - \mu_0(\alpha_2\alpha_3 + 2\alpha_4\alpha_1) + 3\varepsilon_0(\alpha_2\alpha_3 + 2\mu_0\alpha_4 + 3)}{-3\alpha_1 + \mu_0[-\alpha_2\alpha_3 + \alpha_4(\alpha_1 - 3\varepsilon_0)] + 9\varepsilon_0}, \quad (13)$$

$$\xi_{\rm EH} = \frac{9c\mu_0 a_2\varepsilon_0}{-3a_1 + \mu_0[-a_3 a_2 + a_4(a_1 - 3\varepsilon_0)] + 9\varepsilon_0}, \quad (14)$$

$$\xi_{\rm HE} = \frac{9c\mu_0 a_3\varepsilon_0}{-3a_1 + \mu_0[-a_3 a_2 + a_4(a_1 - 3\varepsilon_0)] + 9\varepsilon_0}. \quad (15)$$

In the above derivations, we obtained the expressions for the electric permittivity and magnetic permeability, and the complex chirality coefficients of the atomic media. Substituting Eqs. (12)–(15) into Eq. (2), we can also present the expression for refractive index. In the next section, we will show that the negative refractive index of the atomic system can be obtained without simultaneously requiring both negative permittivity and permeability.

## 3. Results and discussion

Before doing these calculations, we need to fix several key parameters in these equations, such as spontaneous emission rate, wavelength and atomic density. In the model configuration, the transition from state $|2\rangle$ to state $|1\rangle$ is magnetic-dipole allowed and others are electrical-dipole allowed. The typical value of the spontaneous emission rate of atomic electric dipole transitions is the magnitude of $10^8$ Hz. The spontaneous emission rate of atomic magnetic dipole transitions is in general smaller than that of atomic electric dipole transitions by four magnitudes. Thus, in our numerical calculations, the spontaneous emission rates are scaled by $\gamma = 10^8$ s$^{-1}$: $\gamma_{21} = \gamma_{43} \times (1/137)^2$,[20] $\gamma_{31} = \gamma_{42} = \gamma_{\rm c} = 1\gamma$ for simplicity. The typical optical wavelength for the transitions $|4\rangle \to |3\rangle$ and $|2\rangle \to |1\rangle$ is selected to be 600 nm. The dipole moments $d_{12}$ and $\mu_{34}$ are estimated by the relation $\sqrt{3\hbar\Gamma_{ij}\lambda^3/8\pi^2}$. In the present calculations, we choose the density of atoms $N$ to be $5 \times 10^{24}$ m$^{-3}$. Dense vapour is required so that the atomic density should be larger than $10^{24}$ m$^{-3}$.[20] The detuning of the strong signal field is set as $\Delta_{\rm s} = 0$ with Rabi frequency $\Omega_{\rm s} = 20\gamma$. As mentioned previously, the requirement of a strong magnetic-dipole transition and a strong electric-dipole transition near the same transition frequency puts a stringent constraint on the energy level structure of systems where negative refraction can be achieved.[20] In our scheme, the electric-dipole and magnetic-dipole transition occur at different transition frequencies because the magnetic component of the probe field and the control field detunings are assumed to be the same, $\Delta_{\rm m} = \Delta_{\rm c} = 0.001\gamma$.

Figure 2 shows the real and imaginary parts of the chirality coefficients $\xi_{\rm EH}$ and $\xi_{\rm HE}$ as a function of $\Delta_{\rm p}/\gamma$. It is observed that their real and imaginary parts have the same order of magnitude but the opposite phase, simultaneously. A similar conclusion can also be drawn when varying $\Omega_{\rm c} = 0.4\gamma$, $0.8\gamma$, or $\theta = 3\pi/2$, $\Omega_{\rm c} = 1\gamma$, $1.4\gamma$, $1.8\gamma$, respectively. The sum of the two chirality coefficients $\xi_{\rm EH}$ and $\xi_{\rm HE}$ will vanish in Eq. (2). Negative refraction can possibly be obtained when the chirality coefficients are large enough.

In Fig. 3(a), the refractive index is plotted for $\theta = \pi/5$, $\Omega_{\rm c} = 0.4\gamma, 0.8\gamma$, $1.3\gamma$, and the black, gray and light gray curves correspond to the different values of $\Omega_{\rm c}$, respectively. The other parameters are identical to those in Fig. 2. As shown in Fig. 3(a), the real part of the refractive index is negative in the region of [0,2$\gamma$], and the imaginary part depicts the absorption and gain properties. When $\Omega_{\rm c} = 1.3\gamma$, the amplitude of the negative refractive index reaches its maximum. We change the phase difference between the control and pump fields to $\theta = 3\pi/2$ and vary $\Omega_{\rm c}$ by $1\gamma$, $1.4\gamma$, $1.8\gamma$ in Fig. 3(b). It is observed that the negative refractive index amplitude decreases with the variation of $\Omega_{\rm c}$ and the frequency region of the negative refractive index gradually widens with the same variation. The imaginary part of the refractive index shows that some absorptions do exist in the same regions mentioned in Ref. [23], due to the effect of the electro-

magnetically induced chirality.

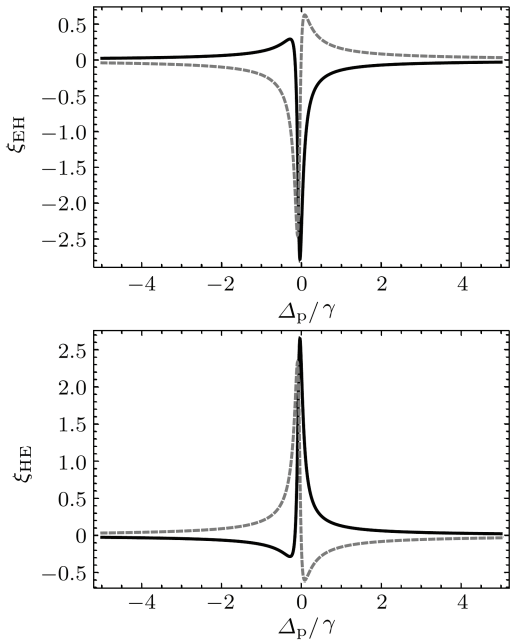



**Fig. 2.** Real (solid lines) and imaginary (dashed lines) parts of the chirality coefficients as a function of the rescaled detuning parameter $\Delta_{\rm p}/\gamma$ for $\theta = \pi/5$, $\Omega_{\rm c} = 1.3\gamma$, and the other parameters are given in the text.

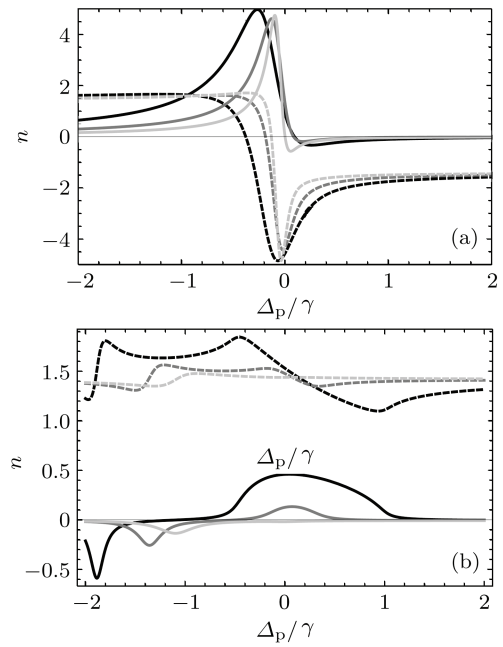



**Fig. 3.** Real (solid lines) and imaginary (dashed lines) parts of the refractive index as a function of the rescaled detuning parameter $\Delta_{\rm p}/\gamma$. The black, gray and light gray lines correspond to different values of $\Omega_{\rm c}$, respectively, for case (a): $\theta = \pi/5$, $\Omega_{\rm c} = 0.4\gamma$, $0.8\gamma$, $1.3\gamma$ and case (b): $\theta = 3\pi/2$, $\Omega_{\rm c} = 1\gamma$, $1.4\gamma$, $1.8\gamma$. The other parameters are the same as those in Fig. 2.

We plot the electric permittivity and magnetic permeability in Fig. 4 by the separate depiction of their real and imaginary parts, respectively. We notice that the electric permittivity and magnetic permeability are not simultaneously negative in the frequency region of negative refraction mentioned in Fig. 3. The real part of electric permittivity is negative in the considered frequency range but the magnetic permeability is not always like this. A similar conclusion can be drawn by varying the corresponding parameters identically to those in Fig. 3.

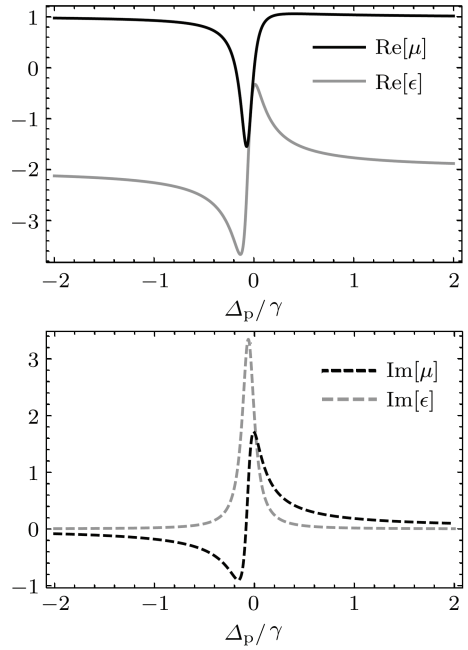



**Fig. 4.** Real (solid lines) and imaginary (dashed lines) parts of permittivity and permeability as a function of the rescaled detuning parameter $\Delta_{\rm p}/\gamma$ for $\theta = \pi/5$, $\Omega_{\rm c} = 1.3\gamma$, the other parameters are the same as those in Fig. 2.

In experimental investigations, the level configuration shown in Fig. 1 may be realized in atomic hydrogen or neon because each has the same level structure as that in Fig. 1.[19] Detailed assessment of our approach in such a system will be our future investigation. We also expect that our technique will be applicable in other systems, such as molecules or solid-state structures.

## 4. Conclusion

In conclusion, we utilized magneto–electric cross coupling to obtain a chirality-induced negative index of refraction without the requirement for simultaneously negative permittivity and permeability. By tuning the phase and amplitude of the external fields properly, the two chirality coefficients have the same amplitude but the opposite phase, and the atomic

system shows that negative refraction can be carried out without requiring the simultaneous presence of an electric-dipole and a magnetic-dipole transition near the same transition frequency.

## References


[1] Veselago V G 1968 *Soviet Physics Usp.* **10** 509

[2] Shelby R, Smith D R and Schultz S 2001 *Science* **292** 77

[3] Yen T J, Padilla W J, Fang N, Vier D C, Smith D R, Pendry J B, Basov D N and Zhang X 2004 *Science* **303** 1494

[4] Veselago V G and Narimanov E E 2006 *Nature Mater.* **5** 759

[5] Chen Y Y, Huang Z M, Shi J L, Li C F and Wang Q 2007 *Chin. Phys.* **16** 173

[6] Zhao S C and Liu Z D 2009 *Int. J. Quantum Information* **7** 747

[7] Lin Z L, Ding J C and Zhang P 2009 *Chin. Phys.* B **18** 954

[8] Pendry J B 2000 *Phys. Rev. Lett.* **85** 3966

[9] Aydin K, Bulu I and Ozbay E 2007 *Appl. Phys. Lett.* **90** 254102

[10] Chen L, He S and Shen L 2004 *Phys. Rev. Lett.* **92** 107404

[11] Jiang Y Y, Shi H Y, Zhang Y Q, Hou C F and Sun X D 2007 *Chin. Phys.* **16** 1959

[12] Dong Z G, Zhu S N and Liu H 2006 *Chin. Phys.* **15** 1772

[13] Shelby R A, Smith D R and Schultz S 2001 *Science* **292** 77

[14] Pendry J B 2003 *Nature* **423** 22

[15] Cubukcu E 2003 *Nature* **423** 604

[16] Eleftheriades G V, Iyer A K and Kremer P C 2002 *IEEE Trans. Microwave Theory Tech.* **50** 2702

[17] Pendry J B 2004 *Science* **306** 1353

[18] Yannopapas V 2006 *J. Phys.*: *Condens. Matter* **18** 6883

[19] Thommen Q and Mandel P 2006 *Phys. Rev. Lett.* **96** 053601

[20] Oktel M Ö and Mütecaplğu ö E 2004 *Phys. Rev.* A **70** 053806

[21] Shen J Q 2006 *Phys. Lett.* A **357** 54

[22] Monzon C and Forester D W 2005 *Phys. Rev. Lett.* **95** 123904

[23] Käastel J, Fleischhauer M, Yelin S F and Walsworth R L 2007 *Phys. Rev. Lett.* **99** 073602

[24] Käastel J, Fleischhauer M and Walsworth R L 2009 *Phys. Rev.* A **79** 063818

[25] Zhao S C, Liu Z D and Wu Q X 2010 *Chin. Phys.* B **19** 014211

[26] Shen J Q 2007 *Chin. Phys.* **16** 1976

[27] Cook D M 1975 *The Theory of the Electromagnetic Field* (New Jersey: Prentice-Hall) Chap. 11

[28] Jackson J D 1999 *Classical Electrodynamics* 3rd edn. (New York: Wiley) p. 160